H1 Preliminary								
$\langle F\rangle$	$\alpha_s(M_Z)$	$\lambda/$ GeV	χ^2_n	$\kappa/\%$	$\alpha_s(M_Z)$	$\mu/$ GeV^2	χ^2_n	$\kappa/\%$
$\langle\tau\rangle$	0.132	-0.04	0.6	-99	0.131	-0.23	0.6	-89
$\langle B\rangle$	0.120	0.53	0.8	-92	0.128	3.07	1.7	-68
$\langle\tau_C\rangle$	0.157	-0.15	1.3	-99	0.154	-0.57	1.1	-86
$\langle\rho\rangle$	0.165	-0.09	0.5	-99	0.161	-0.27	0.4	-87
$\langle C\rangle$	0.161	-1.39	2.0	-99	0.152	-4.84	1.0	-85
$\langle y_{fJ}\rangle$	0.114	-0.08	1.6	-97	0.112	-0.28	1.7	-82
$\langle y_{k_t}\rangle$	0.122	-0.45	1.6	-99	0.105	1.33	1.6	-93

Table 1: Results of two-parameter fits of $\alpha_s(M_Z)$ and simple λ/Q resp. μ/Q^2 power corrections for the event shape means. κ denotes the correlation coefficient between the two fit parameters.

H1 Preliminary					
$\langle F\rangle$	a_F	$\overline{\alpha}_0(\mu_I = 2\,\text{GeV})$	$\alpha_s(M_Z)$	χ^2/n	$\kappa/\%$
$\langle\tau\rangle$	1	$0.480 \pm 0.028\ ^{+0.048}_{-0.062}$	$0.1174 \pm 0.0030\ ^{+0.0097}_{-0.0081}$	0.5	-97
$\langle B\rangle$	$1/2 \cdot a'_B$	$0.491 \pm 0.005\ ^{+0.032}_{-0.036}$	$0.1106 \pm 0.0012\ ^{+0.0060}_{-0.0057}$	0.7	-58
$\langle\tau_C\rangle$	1	$0.475 \pm 0.003\ ^{+0.044}_{-0.048}$	$0.1284 \pm 0.0014\ ^{+0.0100}_{-0.0092}$	1.3	$+19$
$\langle\rho\rangle$	$1/2$	$0.561 \pm 0.004\ ^{+0.051}_{-0.058}$	$0.1347 \pm 0.0015\ ^{+0.0111}_{-0.0100}$	1.2	$+7$
$\langle C\rangle$	$3\pi/2$	$0.425 \pm 0.002\ ^{+0.033}_{-0.039}$	$0.1273 \pm 0.0009\ ^{+0.0104}_{-0.0093}$	0.9	$+63$
$\langle y_{fJ}\rangle$	1	0.258 ± 0.004	0.104 ± 0.002	1.9	-61

Table 2: Results of two-parameter fits of $\overline{\alpha}_0(\mu_I = 2\,\text{GeV})$ and $\alpha_s(M_Z)$ according to the power correction approach initiated by Dokshitzer and Webber for the event shape means. The uncertainties are statistical and total systematic except for y_{fJ} where a coefficient $a_{y_{fJ}}$ different from 1 is anticipated. κ denotes the correlation coefficient between the two fit parameters.

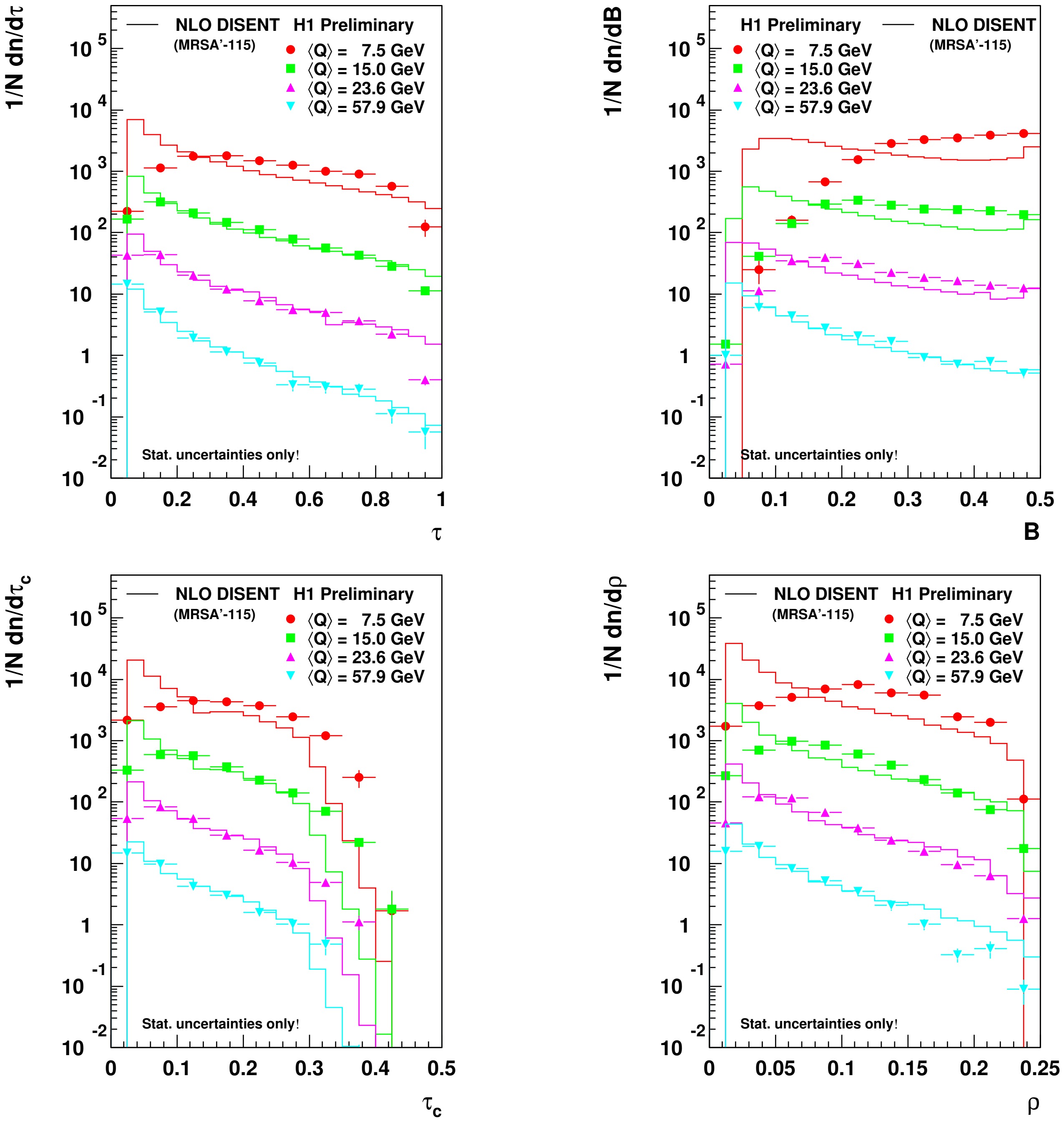

Figure 1: Normalized differential distributions of the event shapes τ, B, τ_C and ρ corrected for detector effects. H1 data (full symbols) are compared with DISENT 0.1 NLO calculations (full lines) for four out of eight investigated bins in Q. The spectra for $\langle Q \rangle = 7.5$–$57.9\,\mathrm{GeV}$ are multiplied by factors of 10^n, $n = 0, 1, 2, 3$. The error bars represent statistical uncertainties only. Note that the range corresponding to the left-most data bin was omitted in the normalization.

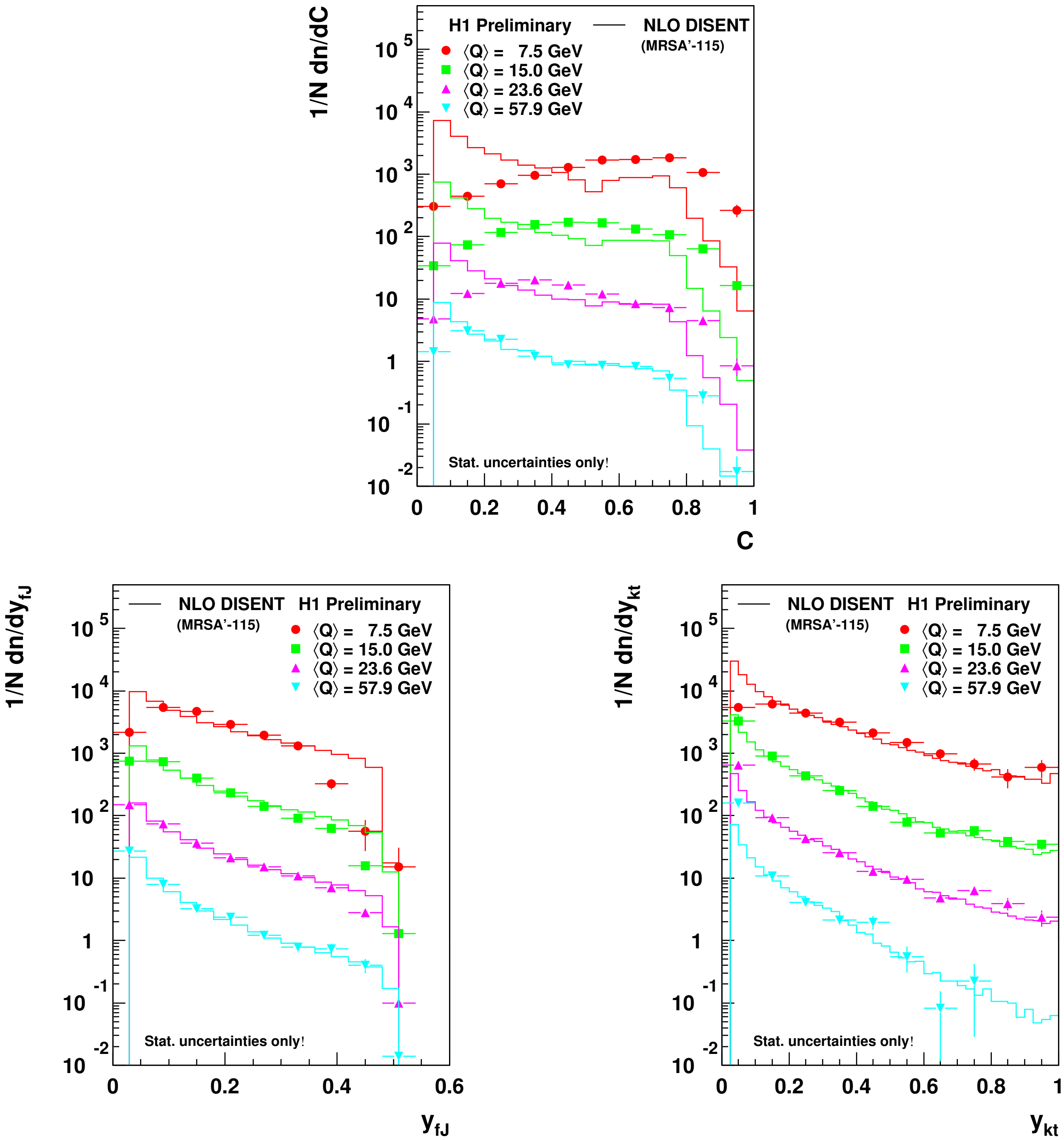

Figure 2: Normalized differential distributions of the event shapes C, y_{fJ} and y_{k_t} corrected for detector effects. H1 data (full symbols) are compared with DISENT 0.1 NLO calculations (full lines) for four out of eight investigated bins in Q. The spectra for $\langle Q \rangle = 7.5$–$57.9\,\mathrm{GeV}$ are multiplied by factors of 10^n, $n = 0, 1, 2, 3$. The error bars represent statistical uncertainties only. Note that the range corresponding to the left-most data bin was omitted in the normalization.

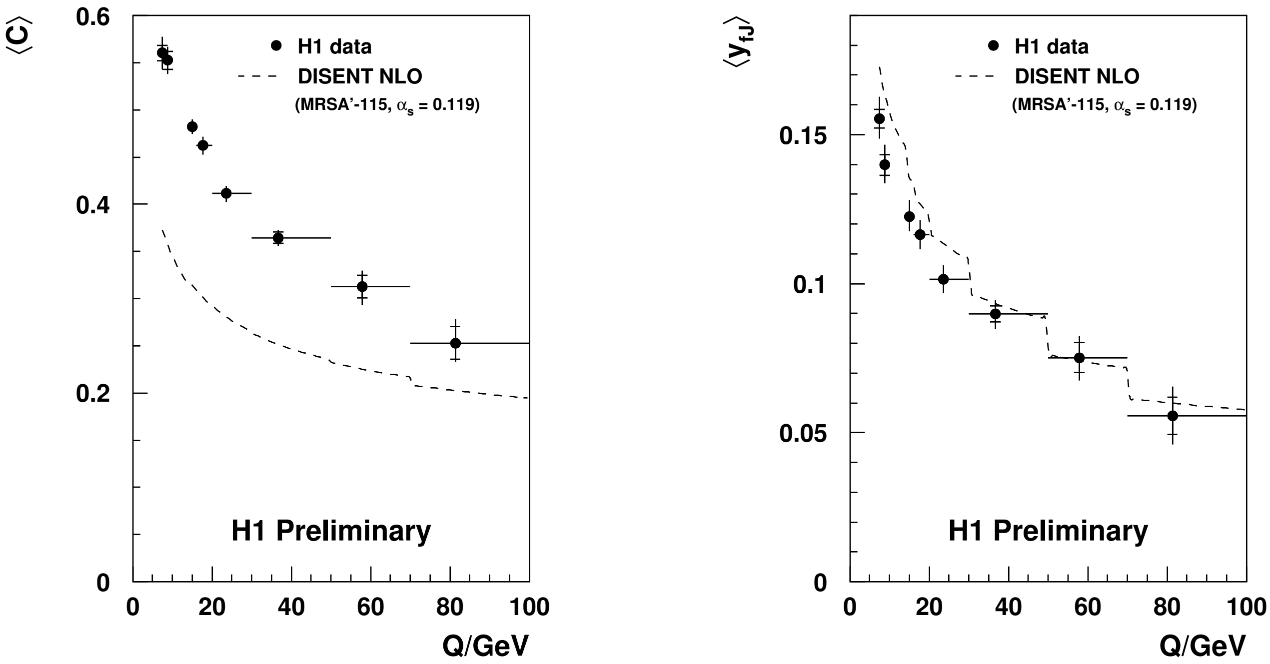

Figure 3: Corrected means (full symbols) of C and y_{fJ} as a function of Q. The inner error bars represent the statistical uncertainty, the outer ones the total statistic and systematic uncertainty. They are compared to DISENT 0.1 NLO calculations with $\alpha_s(M_Z)$ set to 0.119 (dashed lines).

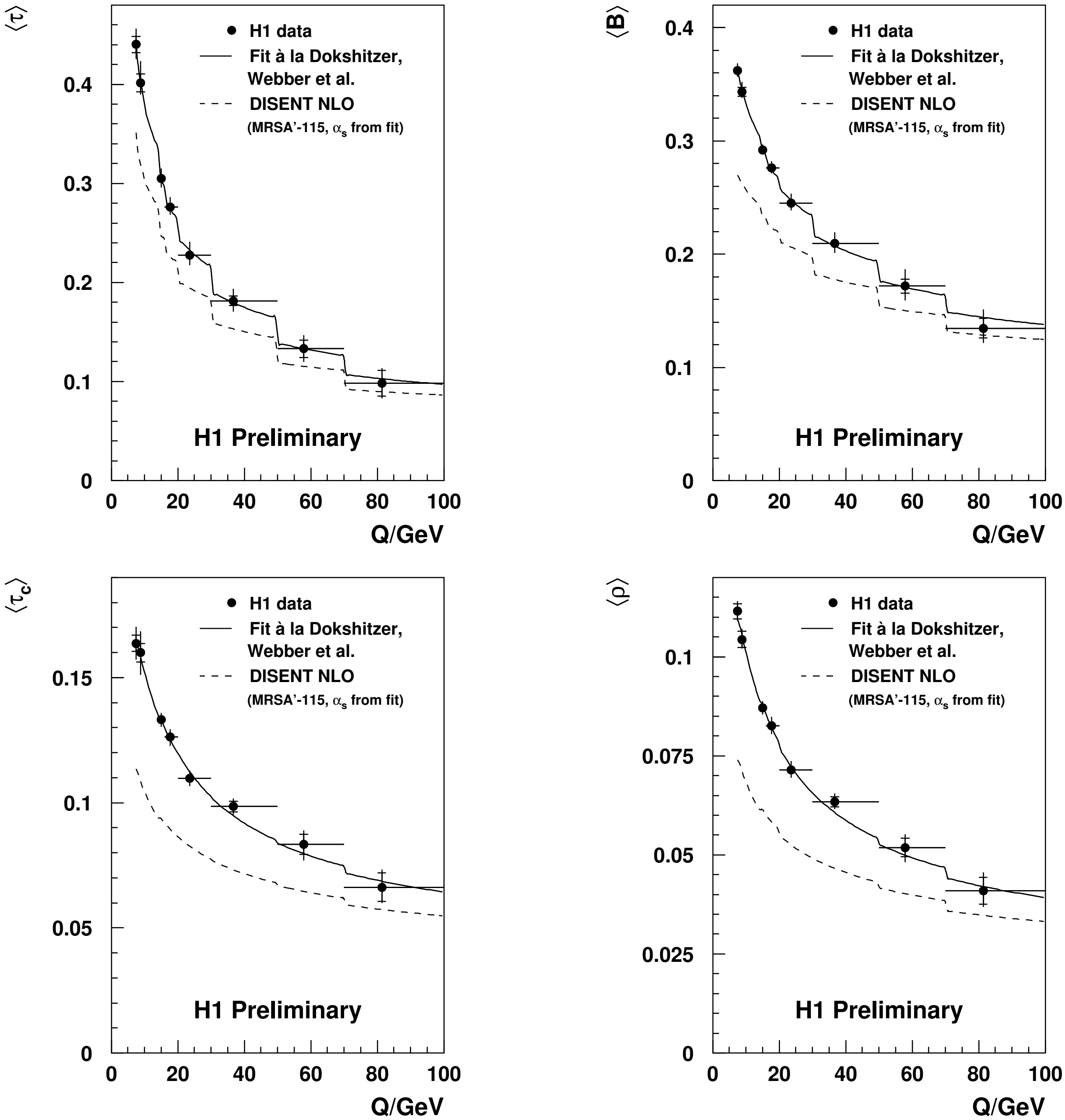

Figure 4: Corrected means (full symbols) of τ, B, τ_C and ρ as a function of Q. The inner error bars represent the statistical uncertainty, the outer ones the total statistic and systematic uncertainty. The full line corresponds to a power correction fit according to the approach initiated by Dokshitzer and Webber. Taking $\alpha_s(M_Z)$ from the fit the NLO prediction of DISENT 0.1 (dashed line) is shown for comparison.

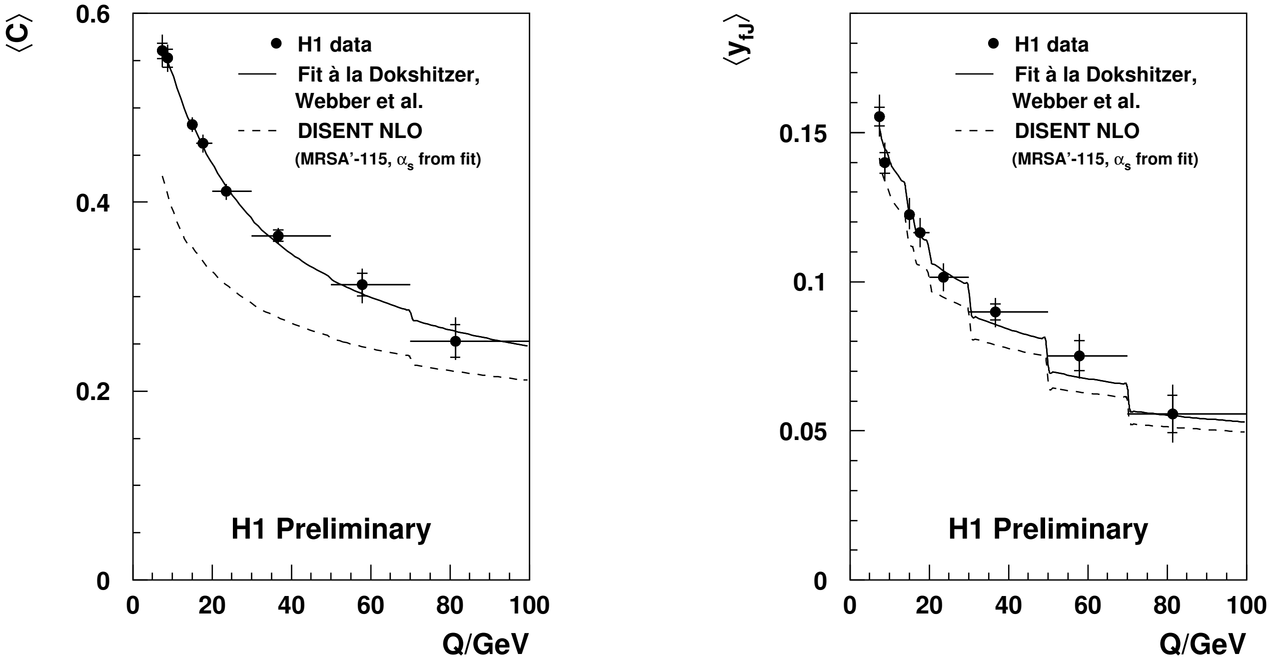

Figure 5: Corrected means (full symbols) of C and y_{fJ} as a function of Q. The inner error bars represent the statistical uncertainty, the outer ones the total statistic and systematic uncertainty. The full line corresponds to a power correction fit according to the approach initiated by Dokshitzer and Webber. Taking $\alpha_s(M_Z)$ from the fit the NLO prediction of DISENT 0.1 (dashed line) is shown for comparison.

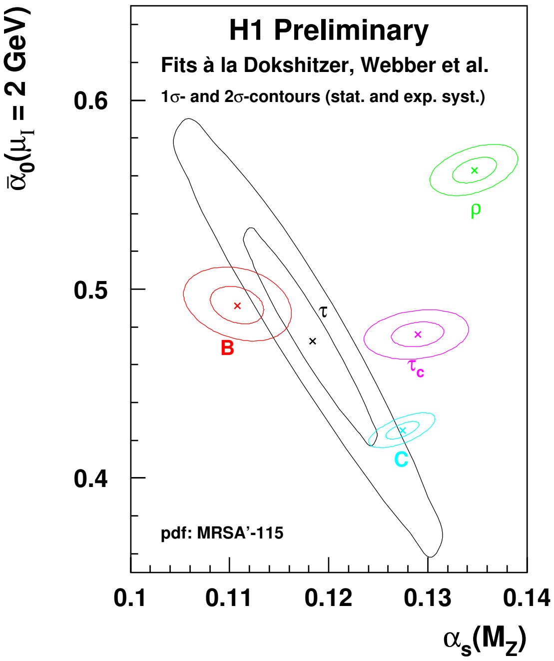

Figure 6: Results of two-parameter power correction fits for the means of τ, B, τ_C, ρ and C in the form of 1σ- and 2σ-contours in the $(\alpha_s, \overline{\alpha}_0)$-plane including statistical and experimental systematic uncertainties.

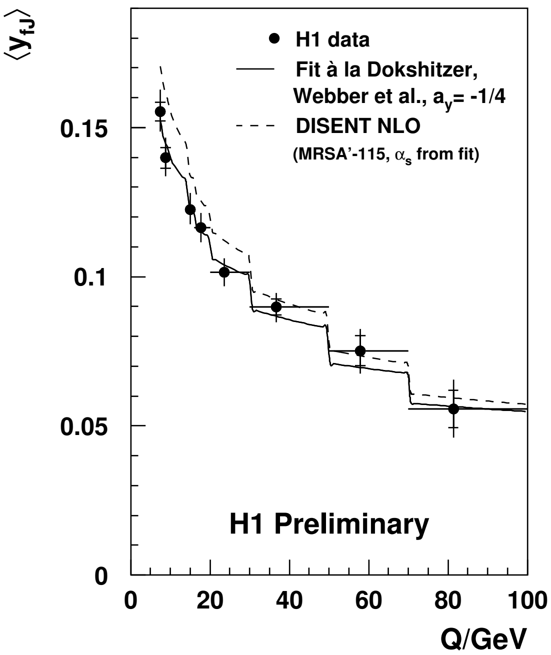

Figure 7: Corrected means (full symbols) of y_{fJ} as a function of Q. The inner error bars represent the statistical uncertainty, the outer ones the total statistic and systematic uncertainty. The full line corresponds to a power correction fit according to the approach initiated by Dokshitzer and Webber with $a_{y_{fJ}}$ set to $-1/4$. Taking $\alpha_s(M_Z)$ from the fit the NLO prediction of DISENT 0.1 (dashed line) is shown for comparison.

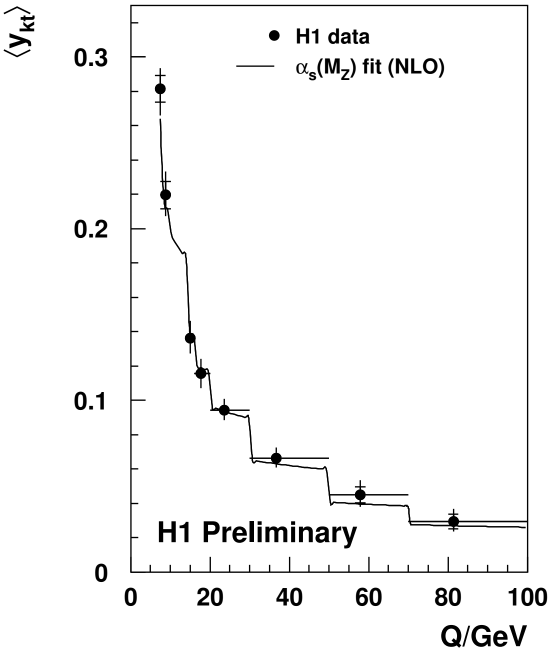

Figure 8: Corrected means (full symbols) of y_{k_t} as a function of Q. The inner error bars represent the statistical uncertainty, the outer ones the total statistic and systematic uncertainty. The full line corresponds to a fit of $\alpha_s(M_Z)$ using the NLO prediction of DISENT 0.1 and assuming that power corrections are negligible.

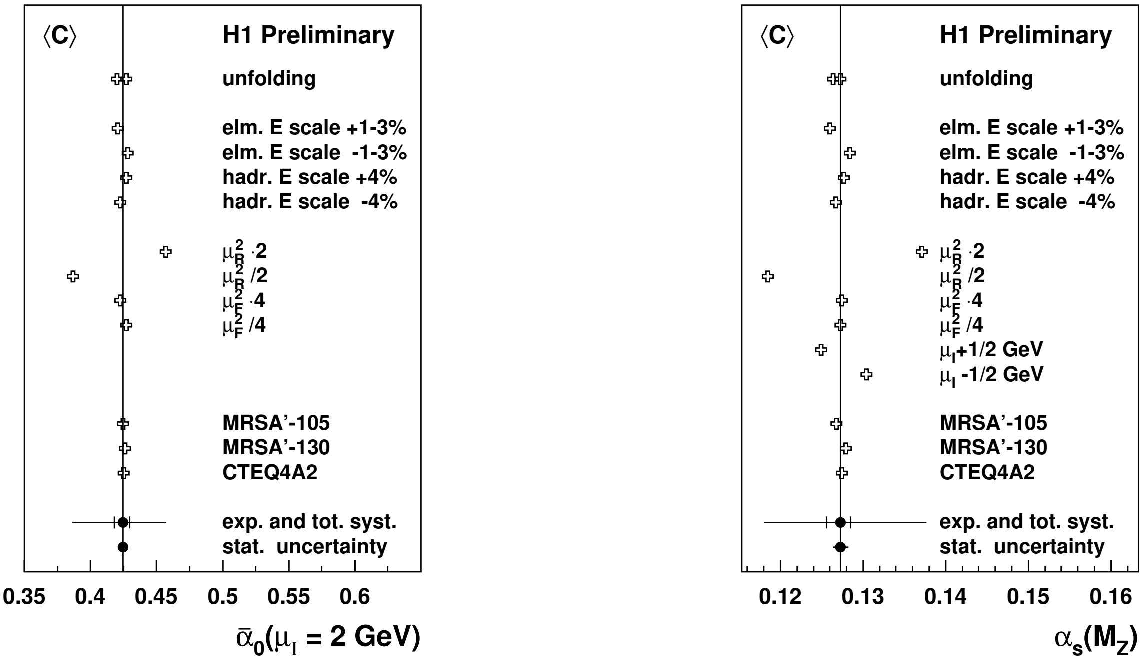

Figure 9: Systematic uncertainties of $\overline{\alpha}_0(\mu_I = 2\,\mathrm{GeV})$ (left) and $\alpha_s(M_Z)$ (right) for C.